



# Mathematical Modeling of Fluid Flow through Channels behind Well Casing

Guo B<sup>1\*</sup>, Cai X<sup>2</sup> and Lee J<sup>1</sup>

<sup>1</sup>University of Louisiana at Lafayette, USA

<sup>2</sup>PetroChina Company, China

\*Corresponding author: Boyun Guo, University of Louisiana at Lafayette, USA, Tel: 2813807616; Email: guo.boyun@gmail.com

Research Article

Volume 4 Issue 4

Received Date: July 25, 2020

Published Date: August 10, 2020

DOI: 10.23880/ppej-16000231

## Abstract

Oil and gas leakage through channels in the annular space of oil and gas wells has long been a problem responsible for sustained casing pressure and environmental issues. This type of channels forms due to low efficiency of cement placement during well cementing processes, gravity segregation after cementing horizontal wells, formation fluid invasion during the setting of cement slurry, and corrosion of formation gas, such as CO<sub>2</sub> and H<sub>2</sub>S over the life of well service. Successful sealing of the channels requires a rigorous hydraulics model for simulating the friction of sealants in the channel. The challenge is from the irregular shape of cross sections of the channels. Owing to the nature of circular shapes of wellbore and casing, bow-shape cross sections are assumed to represent these irregular shapes of cross sections. An analytical model is presented to describe laminar flow in channels of bow-shaped cross sections. The model is validated by a comparison with a traditional rectangular slot model for narrow cross sections. Result of model analysis indicates that use of rectangular cross sections to approximate bow-shaped cross sections will under-estimate the pressure gradient in narrow cross sections and over-estimate the pressure gradient in wide cross sections. A case analysis of a cement squeezing operation shows that the newly developed hydraulics model for fluid flow in channels of bow-shaped cross sections is easy to use in engineering applications.

**Keywords:** Laminar flow; Slot; Cross section; Channel; Pressure; Model

## Introduction

Fluid flow through channels in the cement sheath behind casing in oil and gas wells has long been a problem responsible for gas and oil leakage from gas and oil pay zones to surface or other formation zones, threatening surface and/or environment [1]. This type of channels forms due to low efficiency of cement placement during well cementing processes, gravity segregation after cementing horizontal wells, formation fluid invasion during the setting of cement slurry, and corrosion of formation gas, such as CO<sub>2</sub> and H<sub>2</sub>S over the life of well service [2,3]. Detection and mitigation of the problem have been studied for a decade [4-7].

Squeeze cementing technology has long been available that allowed the first attempt success in mitigation of the flow-behind-casing problem [8]. The squeezing efforts can take days when multiple attempts are necessary. Experiments using various techniques to remedy the problem of flow behind casing have been costly and have consistently had low rates of success. Wireline logging, high density perforating and cement/resin squeezing have been applied. Cement squeezing without damaging formation is virtually impossible due to large cement particles bridging and hydration [9]. The repair of the problem is a non-revenue generating exercise with significant expenditures. The process involves a) identifying the fluid source or sources that are responsible

for the problem and b) communicating with this fluid source in a manner that enhances a remedial cementing activity [10]. There are essentially three areas of squeeze cementing that are generally misunderstood and misapplied. They are 1) injection rates are conducted at excessively high rates and pressures and either create or perpetuate damage, 2) proper design of cement slurry properties is often neglected, and 3) the slurry is placed downhole at too high a rate because of the fear of cementing up a workstring in limited thickening time, which causes excessive formation breakdown, losing cement to the formation. These issues are inter-related through the slurry flow hydraulics in the channels behind the casing.

Effective mitigation of the problem requires adequate mathematical modeling of fluid movement behind casing [11]. However, such mathematical modeling work has not been done. Result of modeling should allow for selection of choice of treatment method, properties of blocking agent/material, volume of blocking agent/material to be used, and placement method.

Owing to the nature of radial geometry of wellbore, it is expected the cross section of the channels in general takes an arc shape in one side and a near-straight shape in the other side, or bow-shape. Figure 1 presents images of channels in cement sheath observed by Goodwin and Crook in laboratory [12]. It indicates that the cross-section of wide channels such as that shown in Figure 1(a) can be approximated by a bow shape, while that of narrow channels shown in Figure 1(b) may be approximated by slots.

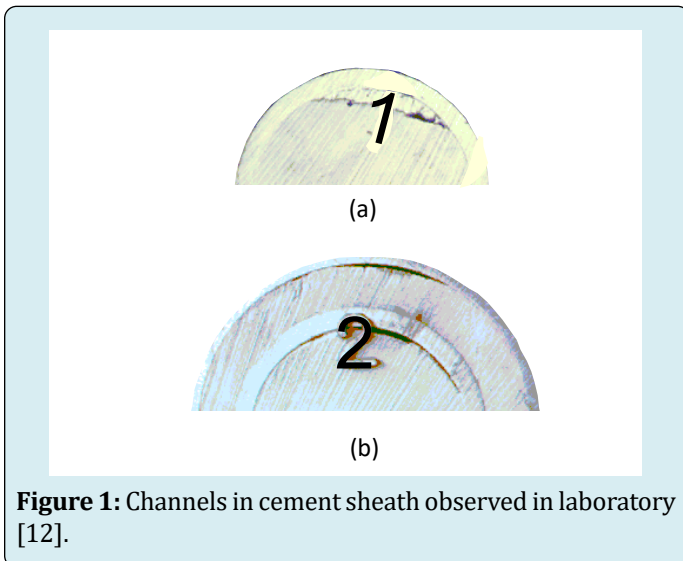


**Figure 1:** Channels in cement sheath observed in laboratory [12].

Figure 2 shows a schematic of an idealized cross section of a water channel in the cement sheath. Mathematical modeling of fluid flow in channels with bow-shape cross-sections is not available from literature. But a method of solving similar

flow problems with other irregular cross sections is found. Tamayol and Bahrami [13] presented analytical solutions for a fully developed laminar flow through hyper-elliptical and polygonal microchannels. The presented model enables the prediction of velocity distribution and pressure drop for several common fabricated geometries for industrial applications including circular, elliptical, rectangular, rhombus, triangular, and hexagonal ducts. Model-predicted values were successfully compared with experimental data collected by others for rectangular channels. Wu [14] performed a comprehensive investigation of the influence of cross-sectional shapes on channel flow. The cross-sectional shapes that he studied are circle, rectangle, ellipse, eccentric annulus, half-moon, circular sector, equilateral triangle, and limaçon. The most popular model used in the oil and gas industry is still Bourgoyne, et al. [15] model for channels with cross sections of rectangular slot-shape, which is in question for accuracy when applied to channels with cross sections of bow-shape.

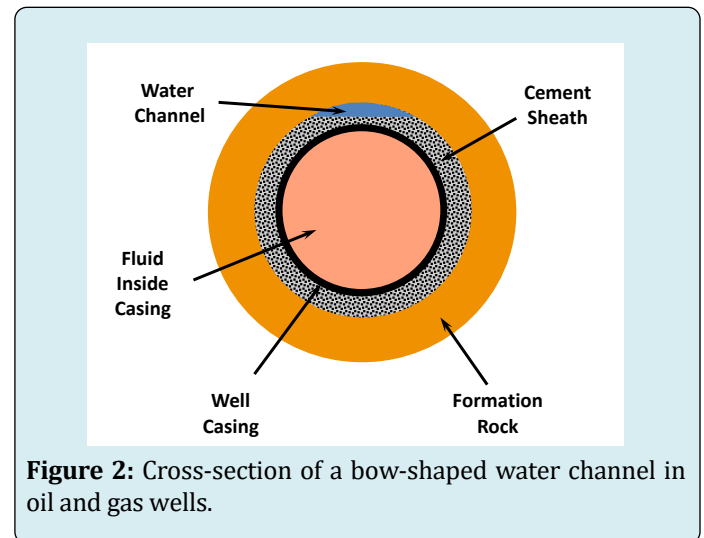


**Figure 2:** Cross-section of a bow-shaped water channel in oil and gas wells.

No study is found from the literature on the fluid flow in channels with bow-shaped cross-sections. This work presents an analytical model for the laminar flow of Newtonian fluids through channels with bow-shaped cross-sections and extends the model to non-Newtonian fluids using apparent Newtonian viscosity. The cross-section is a bow-segment of an oval/ellipse so that bow-segments of circles ( $a=b$ ) and narrow slots ( $a \gg b$ ) are covered.

### Mathematical Model

The standard equation to describe a planar ellipse shown in Figure 3 is written as

$$\frac{x^2}{a^2} + \frac{y^2}{b^2} = 1 \quad (1)$$

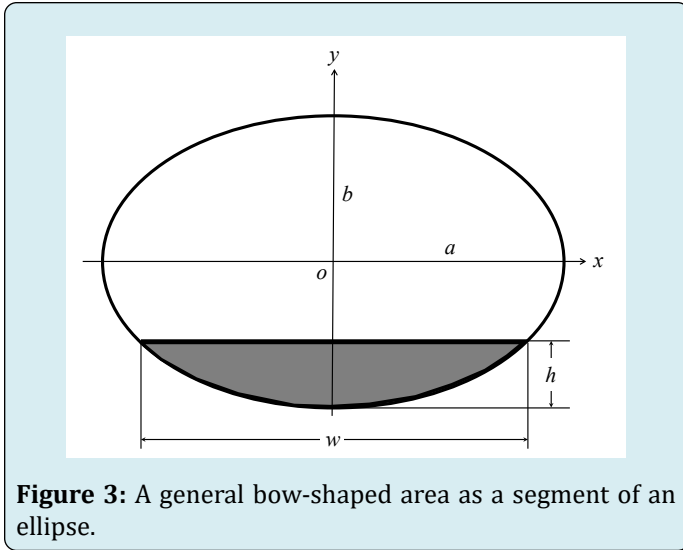


**Figure 3:** A general bow-shaped area as a segment of an ellipse.

The shaded area presents a bow-segment of the ellipse with width  $w$  and height  $h$ . **Appendix A** shows that the area of the bow-segment takes the following form:

$$A = \frac{a}{b} \left[ \frac{\pi}{2} b^2 + (h-b) \sqrt{2hb - h^2} + b^2 \arcsin\left(\frac{h-b}{b}\right) \right] \quad (2)$$

For a special case where  $a=b$ , Equation (2) degenerates to describing a bow-segment of a circular area. Although Equation (2) is derived for a bow-shape segment, it is valid for other shapes of areas as long as the parameter  $h$  takes values between  $0$  and  $2b$ . Table 1 lists some special shapes of areas with  $h=b/2$ ,  $h=b$ ,  $h=3/2b$ , and  $h=2b$  for  $a=b$ ,  $a=2b$ , and  $a \gg b$ .

	$h = b/2$	$h = b$	$h = 3b/2$	$h = 2b$
$a = b$				
$a = 2b$				
$a \gg b$				

**Table 1:** Some Special Shapes of Segment Areas for Various  $a$  and  $h$  Values.

For the total volumetric flow rate  $Q$ , the mean flow velocity through the cross section is expressed in consistent units as

$$v_{av} = \frac{Q}{A} = \frac{b}{a \left[ \frac{\pi}{2} b^2 + (h-b) \sqrt{2hb - h^2} + b^2 \arcsin\left(\frac{h-b}{b}\right) \right]} \quad (3)$$

The expression for the frictional pressure gradient of laminar flow through the channel is derived in Appendix B. The resultant solution takes the following form:

$$\frac{dp_f}{dz} = \frac{\mu v_{av}}{1,000 h^2} \quad (4)$$

where  $dp_f/dz$  is frictional pressure gradient in psi/ft,  $\mu$

is Newtonian viscosity in cp,  $v_{av}$  is the mean flow velocity in ft/s, and  $h$  is height of cross section in inch. Equation (5) is valid for Newtonian fluids only. For non-Newtonian fluids, the Newtonian viscosity  $\mu$  is replaced by the apparent Newtonian viscosity  $m_a$  [16]. For Bingham plastic fluids, the apparent Newtonian viscosity is expressed as

$$\mu_a = \mu_p + \frac{5\tau_y h}{v_{av}} \quad (5)$$

where  $m_a$  is apparent viscosity in cp,  $m_p$  is plastic viscosity in cp, and  $\tau_y$  is yield point in lbf/100ft<sup>2</sup>.

For Power Law fluids, the apparent Newtonian viscosity is expressed as

$$\mu_a = \frac{Kh^{1-n}}{144v_{av}^{1-n}} \left( \frac{2+1/n}{0.0208} \right)^n \quad (6)$$

where  $K$  is consistency index in cp equivalent and  $n$  is flow behavior index.

### Comparison with Other Model

The newly developed model for a channel of bow-shape cross section is compared here with the model presented by Bourgoyne, et al. [15] for a channel of rectangular slot-cross section. The height of the rectangular slot section is taken as the same of the bow-shape cross section  $h$ . The width of the rectangular slot section  $w$  is taken as the width value of the bow-shape section at height  $h$ , according to Equation (7):

$$w = \frac{2a}{b} \sqrt{2bh - h^2} \quad (7)$$

The difference between the two models is expressed by the resistance ratio ( $R_R$ ) defined by:

$$R_R = \frac{\text{Pressure gradient given by Equation (4) for bow-shape cross section}}{\text{Pressure gradient given by Bourgoyne, et al. [15] model for slot-cross section}} \quad (8)$$

where mathematically expressed as:

$$R_R = \frac{w}{w_{eq}} = \frac{\frac{2a}{b} \sqrt{2bh - h^2}}{\frac{a}{hb} \left[ \frac{\pi}{2} b^2 + (h-b) \sqrt{b^2 - (h-b)^2} + b^2 \arcsin \left( \frac{h-b}{b} \right) \right]} \quad (9)$$

or simplified to:

$$R_R = \frac{2 \left( \frac{h}{b} \right) \sqrt{2 \left( \frac{h}{b} \right) - \left( \frac{h}{b} \right)^2}}{\frac{\pi}{2} + \left( \frac{h}{b} - 1 \right) \sqrt{2 \left( \frac{h}{b} \right) - \left( \frac{h}{b} \right)^2} + \arcsin \left( \frac{h}{b} - 1 \right)} \quad (10)$$

It is noticed that the ratio  $R_R$  is independent of  $a$  and  $b$  but  $h/b$  only. Table 2 and Figure 4 present the  $R_R$  data in the full range of  $h/b$ . They indicate that  $R_R=1$  occurs at  $h/b=1.54$ . Figure 5 shows the two cross sections for  $h/b=1.54$ . Since  $R_R=1$  does not hold true at other  $h/b$  ratio values, Bourgoyne, et al. [15] slot cross-section model is not valid for channels with bow-shaped cross sections. The error of Bourgoyne et al.'s model is expressed as

$$E_B = \frac{\Delta p_{slot} - \Delta p_{bow}}{\Delta p_{bow}} = \frac{1}{\frac{\Delta p_{bow}}{\Delta p_{slot}}} - 1 = \frac{1}{R_R} - 1 \quad (11)$$

where  $E_B$  is the relative error of Bourgoyne et al.'s model,  $Dp_{slot}$  is the pressure gradient given by Bourgoyne et al.'s model [15], and  $Dp_{bow}$  is the pressure gradient given by Equation (4). For channels with flat cross sections where  $h/b < 1.0$ , the  $R_R$  value varies from 1.27 to 1.50. These  $R_R$  values are translated by Equation (11) to -21% and -33% relative error, respectively.

h/b	RR	h/b	RR
0.1	1.5	1.55	0.99
0.2	1.48	1.56	0.98
0.3	1.45	1.59	0.96
0.4	1.43	1.62	0.93
0.5	1.41	1.67	0.89
0.6	1.39	1.72	0.83
0.7	1.36	1.77	0.77
0.8	1.34	1.82	0.69
0.9	1.31	1.87	0.6
1	1.27	1.92	0.49
1.1	1.24	1.93	0.46
1.2	1.2	1.94	0.43
1.3	1.15	1.95	0.39
1.4	1.09	1.96	0.35
1.45	1.06	1.97	0.31
1.5	1.03	1.98	0.25
1.51	1.02	1.99	0.22
1.52	1.01	1.99	0.18
1.53	1.01	2	0.13
1.54	1	2	0

**Table 2:** Model-calculated data of  $h/b$  versus  $R_R$

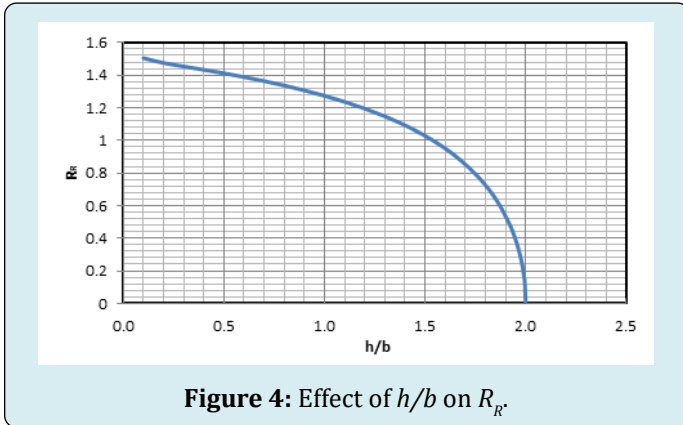


Figure 4: Effect of  $h/b$  on  $R_R$

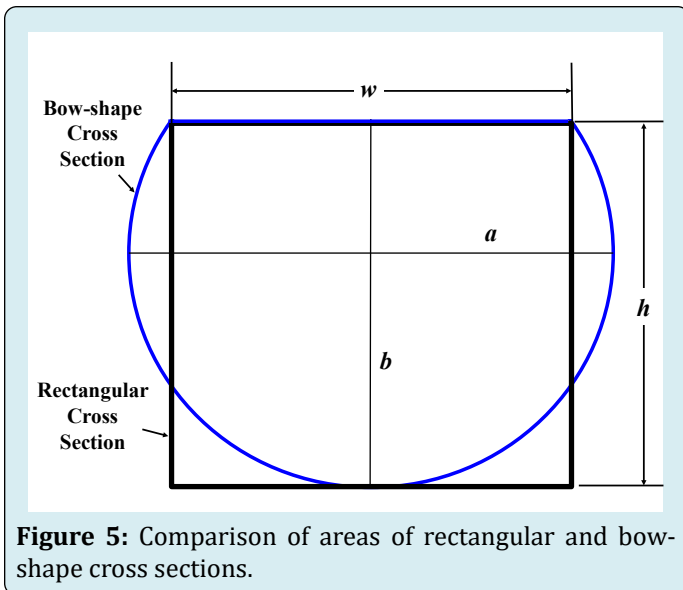


Figure 5: Comparison of areas of rectangular and bow-shape cross sections.

### Case Analysis

This section shows an application of the newly developed hydraulics model in a cement squeezing operation. The objective is to seal a channel behind casing without break down the formation.

A primary cement job has been performed on a 7" production casing. After 48 hours wait on cement time, a cement bond log was run. Result of log interpretation indicated that a long channel exists in the annulus. The volume of the channel is about 5% of the annulus space over the logged interval. A cement squeezing operation is designed as shown in Figure 6. The cement slurry is designed to have a weight of 15.8 ppg with flow consistency  $K=30$  cp equivalent and flow behavior index  $n=0.95$ . The placement efficiency of cement in the channel depends on cement properties and cement slurry flow velocity during cement squeezing. It is essential to know the maximum permissible pumping rate that will not induce friction pressure to break down the formation. It is also essential to know the peak surface pumping pressure

corresponding to the formation fracturing pressure at bottom hole so that the pumping rate is monitored and controlled to avoid formation break down.

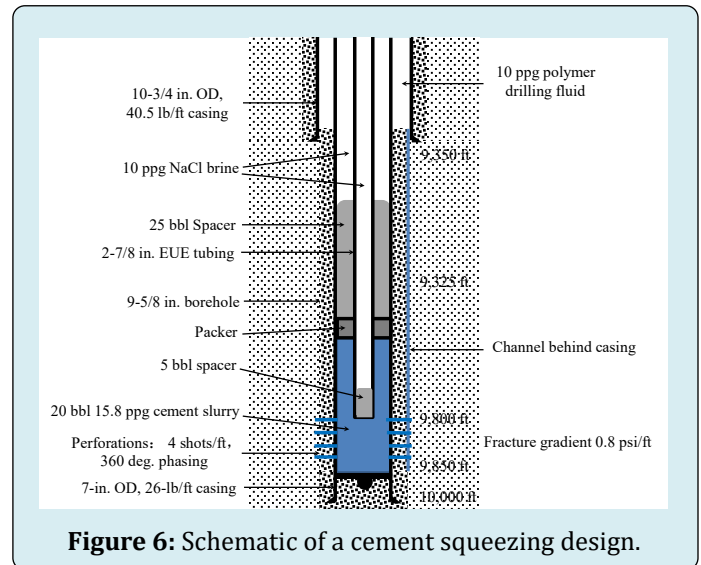


Figure 6: Schematic of a cement squeezing design.

The annulus area is

$$A_a = \frac{\pi}{4} \left[ (9.625)^2 - (7)^2 \right] = 32.26 \text{ in}^2$$

The cross sectional area of the channel is estimated to be  $(0.05)(34.26) = 1.71 \text{ in}^2$

Assuming bow-shape cross section of the channel, the height of the cross section can be estimated using Equation (2):

$$1.71 = \frac{9.625/2}{9.625/2} \left[ \frac{\pi}{2} (9.625/2)^2 + (h - 9.625/2) \sqrt{2h(9.625/2) - h^2} + (9.625/2)^2 \arcsin \left( \frac{h - 9.625/2}{9.625/2} \right) \right]$$

which gives  $h = 0.57$  in.

The formation fracturing pressure can be predicted using formation fracture pressure gradient 0.8 psi/ft and depth at the bottom of channel:

$$p_F = (0.8)(9,850) = 6,304 \text{ psi}$$

The flowing cement pressure at the bottom of the channel is:

$$p_C = (0.052)(10)(9,350) + (0.052)(15.8)(9,850 - 9,350) + p_f \\ = 5,273 + p_f$$

Equating  $P_F$  and  $P_C$  yields maximum permissible friction pressure of cement slurry  $p_f = 1,031$  psi, which gives pressure gradient of  $dp_f/dz = (1,031)/(9,850 - 9,350) = 2.06$  psi/ft. Table 3 presents a summary of calculations given by Equation

(4). It shows that the maximum permissible pumping rate is 4.33 bpm. For safe operations the cement pressure should be controlled to be lower than the formation breakdown pressure by at least 500 psi. Therefore a pumping rate of 2 bpm is recommended for this operation. This pumping rate is expected to create a frictional pressure of 495 psi in the channel, as shown in Table 3.

Q (bpm)	vav (ft/s)	ma (cp)	d <sub>pf</sub> /dz (psi/ft)	pf (psi)
0.5	3.9	21.6	0.27	133
1	7.9	20.9	0.51	256
1.5	11.8	20.5	0.75	376
2	15.7	20.2	0.99	495
2.5	19.7	20	1.22	612
3	23.6	19.8	1.45	727
3.5	27.5	19.6	1.68	842
4	31.5	19.5	1.91	956
4.33	34.1	19.4	2.06	1,031
4.5	35.4	19.4	2.14	1,069
5	39.3	19.3	2.36	1,181

**Table 3:** Result of Calculations Given by Equation (4).

When the frictional pressure of 495 psi is added to the hydrostatic pressure in the channel, the pressure at the bottom of the channel becomes  $5,273+495=5,768$  psi. This corresponds to a surface squeezing pressure of  $5,768-0.052(10)(9,850) = 646$  psi. The surface "breakdown" pressure is calculated to be

$$p_{bd} = (0.8)(9,850) - (0.052)(10)(9,850) = 2,758 \text{ psi}$$

This pressure is the optimum breakdown pressure. Breakdown can occur at lower pressures depending on the number of opened perforations, increased efficiency with higher viscosity, etc.

## Conclusions

A new analytical model was developed in this project to describe fluid flow in channels behind well casing. The model assumes general bow-shaped cross sections of flow channels. The following conclusions are drawn.

1. The new model is equivalent to the Bourgoyne, et al. [15] slot model only for channel parameter  $h/b=1.54$ , indicating a limitation of Bourgoyne, et al. model to channels with special geometries. For channel parameter  $h/b<1.54$ , use of Bourgoyne, et al. model should underestimate pressure gradient in channels; while for channel

parameter  $h/b>1.54$ , use of Bourgoyne, et al. model should over-estimate pressure gradient in channels [15].

2. For channels with narrow cross sections ( $h/b<1$ ) normally found in oil and gas wells, use of the new model should improve accuracy of pressure gradient prediction by 21% to 33% as compared to Bourgoyne, et al. model [15].
3. A case analysis of a cement squeezing operation shows that the newly developed hydraulics model for fluid flow in channels of bow-shaped cross sections is easy to use in engineering applications. However, accurate determination of channel height  $h$  from cement bonding logs is essential to model applications.

## Nomenclature

$A$	= area of bow-shaped cross-sections, in <sup>2</sup>
$a$	= half-length of the long axis of the ellipse, in
$b$	= half-length of the short axis of the ellipse, in
$F_1$	= force applied by the fluid pressure at Point 1, pound
$F_2$	= force applied by the fluid pressure at Point 2, pound
$F_3$	= frictional force exerted by the adjacent layer of fluid below the fluid element of interest, pound
$F_4$	= frictional force exerted by the adjacent layer of fluid above the fluid element of interest, pound
$h$	= height of bow-shaped cross-section, in
$K$	= fluid consistency index, cp equivalent
$n$	= flow behavior index
$p$	= pressure, pound per square inch (psi)
$p_f$	= frictional pressure, psi
$p_F$	= formation fracturing pressure, psi
$p_c$	= flowing cement pressure at the bottom of the channel, psi
$p_{bd}$	= surface "breakdown" pressure, psi
$Q$	= volumetric flow rate, ft <sup>3</sup> /s
$R$	= radius of the circle, in
$R_R$	= resistance ratio
$v$	= flow velocity, ft/s
$v_{av}$	= average velocity, ft/s
$v_o$	= velocity at boundary, ft/s
$w$	= width of cross-section, in
$w_{eq}$	= equivalent width of cross section, in
$x$	= horizontal coordinate of ellipse

$y$	= vertical coordinate of ellipse
$Dy$	= thickness of fluid element, in
$z$	= horizontal coordinate in the flow direction
$Dz$	= length of the fluid element, in Greeks
$\gamma$	= shear rate, $s^{-1}$
$m$	= Newtonian viscosity, cp
$m_a$	= apparent viscosity, cp
$m_p$	= plastic viscosity, cp
$\tau$	= shear stress, $lb/ft^2$
$t_o$	= shear stress at boundary, $lb/ft^2$
$t_y$	= yield point, $lb/100 ft^2$

### Acknowledgment

This research was supported by the U.S. - Israel Center of Excellence in Energy, Engineering and Water Technology through the project "Safe, sustainable, and resilient development of offshore reservoirs and natural gas upgrading through innovative science and technology: Gulf of Mexico - Mediterranean."

### References

- Uswak G, Howes E (1992) Direct Detection of Water Flow behind Pipe Using A Transient Oxygen Activation Technique. *Journal of Canadian Petroleum Technology* 31(4): 9.
- Dossary A, Al-Majed AA, Hossain E, Rahman MK, Jennings SS, et al. (2011) Cementing at High Pressure Zones in KSA "Discovering the Mystery Behind the Pipe." SPE Middle East Oil and Gas Show and Conference, Society of Petroleum Engineers, Manama, Bahrain, pp: 13.
- Duguid A, Guo B, Nygaard R (2017) Well integrity assessment of monitoring wells at an active  $CO_2$ -EOR flood. 13th International Conference on Greenhouse Gas Control Technologies (GHGT-13), Lausanne, Switzerland, pp: 5119-5138.
- Marca C (1990) 13 Remedial Cementing. *Developments in Petroleum Science* 28: 13-1-13-28.
- Bakulin A, Korneev V (2007) Acoustic Signatures of Cross-flow Behind Casing: Downhole Monitoring Experiment At Teapot Dome. Society of Exploration Geophysicists, San Antonio, Texas.
- Perrier S (2011) Detection of Cross-flows Behind Casing before Perforations, and Cement Isolation Diagnosis Based on Temperature Analysis (TUNU field, Indonesia). International Petroleum Technology Conference. Bangkok, Thailand, pp: 19.
- Croon M, Huber P, Wright J (2019) Enhanced Well Remedial Decisions from Exact Location of Fluid Movement Behind Casing Identification. Abu Dhabi International Petroleum Exhibition & Conference, Society of Petroleum Engineers, Abu Dhabi, UAE, pp: 16.
- Grant WH, White RL, Smith RC, Miller AG (1990) Successful Squeezing of Shallow and Low-Pressure Formations. IADC/SPE Drilling Conference, Society of Petroleum Engineers, Houston, Texas, pp: 8.
- Saponja J (1999) Surface Casing Vent Flow And Gas Migration Remedial Elimination-New Technique Proves Economic And Highly Successful. Petroleum Society of Canada, Calgary, Alberta, pp: 17.
- Slater HJ (2010) The Recommended Practice for Surface Casing Vent Flow and Gas Migration Intervention. SPE Annual Technical Conference and Exhibition, Society of Petroleum Engineers, Florence, Italy.
- Jabarov KA (2019) Mathematical modeling the processes of behind-casing fluid movement in the wells during waiting on cement (Russian). *Oil Industry Journal* 2019(5): 5.
- Goodwin KJ, Crook RJ (1992) Cement Sheath Stress Failure. *SPE Drill Eng* 7(4): 291-296.
- Tamayol A, Bahrami M (2010) Laminar Flow in Microchannels With Noncircular Cross Section. *Journal of Fluids Engineering* 132(11): 111201.
- Wu B (2014) The influence of the cross section shape on channel flow: modeling, simulation and experiment. *Modeling and Simulation*. Université de Grenoble, France, pp: 252.
- Bourgoyne AT, Millheim KK, Chenevert ME, Young FS (1986) Applied Drilling Engineering. Volume 2, SPE textbook series, Society of Petroleum Engineers, Richardson, Texas, USA, pp: 137-144.
- Guo B, Liu G (2011) Applied Drilling Circulation Systems. Gulf Professional Publishing, Elsevier, pp: 272.

